In this study, we examined the release profiles of each component of the nanoparticles in vitro and the residence period of the nanoparticles in the inflammatory lesion in vivo. It is necessary to expand the scale of preparation and standardize the protocol for the industrial manufacture of these nanoparticles for the use of these nanoparticles as pharmaceutical agents. Hence, we prepared the nanoparticles on a large-scale and the ingredients in the resulting formulation were evaluated. In addition, we assessed the long-term stability of freeze-dried nanoparticles during storage at various temperatures.

2. Materials and methods

2.1. Materials

PLA was purchased from Wako Pure Chemicals Industries, Ltd. (Osaka, Japan). The molecular weight of the polymer was determined by gel permeation chromatography as reported before (Ishihara et al., 2009a). PLA with an average Mw of 6170 was used in this study. PEG-PLA was synthesized by ring-opening polymerization of D,L-lactide (Purac America, IL) in the presence of monomethoxy-PEG (Mw: 5580; NOF Co., Tokyo, Japan) (Riley et al., 2001). The composition and molecular weight of the block copolymers were evaluated by ^{1}H NMR and gel permeation chromatography (Ishihara et al., 2009a). PEG-PLA with an average Mw of 15,010 was used in this study. PEG-PLA with a terminal carboxyl group was similarly synthesized using alpha-hydroxy-omega-carboxy PEG (OH-PEG-COOH, Mw: 3640) (Laysan Bio, Arab, AL). The resulting COOH-PEG-PLA was labeled with 4-(aminomethyl)fluorescein (Wako) by condensation with 1-ethyl-3-(3-dimethylaminopropyl) carbodiimide hydrochloride and 4-(dimethylamino)-pyridine in DMSO. The average molecular weight of resulting fluorescein-PEG-PLA was calculated as 15,700 (Mw) by gel permeation chromatography. Spectral analysis showed that the polymer contained 39 nmol of fluorescein in 1 mg. BP and diethanolamine (DEA) were purchased from Sigma–Aldrich (St. Louis, MO). Zinc chloride and polysorbate 80 (Tween 80) were purchased from Wako. A time-resolved fluoroimmunoassay (TR-FIA) kit for betamethasone was supplied by Shionogi & Co., Ltd. (Osaka, Japan). Cy7-dodecylamine conjugate was synthesized by mixing Cy7 mono-N-hydroxy succinimide ester (GE Healthcare, Chalfont St. Giles, UK), dodecylamine and 4-(dimethylamino)-pyridine in DMSO and purified by HPLC (Ishihara et al., 2008, 2009c).

2.2. Preparation of nanoparticles

In this study, nanoparticles with the highest anti-inflammatory activity were prepared by the oil-in-water solvent diffusion method as reported previously (Ishihara et al., 2009b,c). In brief, a mixture of 7.8 mg PEG-PLA and 42.2 mg PLA was dissolved in 1 ml of acetone. To this solution, 500 μl of an acetone solution of DEA (15 mg/ml), followed by 68 μl of an aqueous solution of zinc chloride (1 M; pH 1.9), and then 28 μl of an aqueous solution of BP (350 mg/ml) were added; the mixture was then allowed to stand for 30 min at room temperature. To 25 ml of distilled water stirred at 1000 rpm, the mixture was added dropwise at the rate of 48 ml/h using a 26G needle. A combination of 1 ml of 0.5 M citrate (pH 7.0) aqueous solution and 125 μl of 200 mg/ml polysorbate 80 aqueous solution was immediately added. The nanoparticles were purified and concentrated by ultrafiltration (Centriprep YM-50, Millipore, Bedford, MA). Finally, the nanoparticles were sterilized by filtration through a 0.2-μm re-generated cellulose membrane (Minisart RC, Sartorius AG, Goettingen, Germany). Nanoparticles with dyes (fluorescein and Cy7) were similarly prepared by mixing 1 mg of fluorescein-PEG-PLA and Cy7-dodecylamine conjugate, respectively (Ishihara et al., 2009c).

The preparation of the nanoparticles was scaled up 800-fold in a similar manner. The mixture of 6.2 g PEG-PLA, 33.8 g PLA and 6 g DEA was dissolved in 1200 ml of acetone. To this acetone solution, 53 ml of 1 M zinc chloride aqueous solution (pH 1.9), and BP aqueous solution (6 g in 17 ml water) were added in order. After 30 min, the solution was added to 20 l of distilled water stirred at 1000 rpm with magnetic stirrer, at the rate of 40 l/h through a glass tube with 6.4 mm internal diameter. For the large-scale production of nanoparticles, the rate of acetone addition and the rate of water stirring were optimized, as mentioned above. Next, 1 l of 0.4% polysorbate 80 in 200 mM citrate buffer (pH 7.0) was added to the resulting nanoparticles suspension. The nanoparticles were purified from unencapsulated BP using polyethersulfone ultrafiltration slice cassettes (MWCO: 300 kDa, Sartorius) and then concentrated. The concentrated suspension (700 ml) was sterilized by filtration through a 0.2-μm filter. Finally, the nanoparticle suspension and the aqueous sucrose solution (270 mg/ml) were mixed to attain a final sucrose concentration of 90 mg/ml. The suspension in each vial was frozen at −50 °C for 4 h on the shelf and freeze-dried through primary step (shelf temperature −20 °C, chamber pressure 25 mT, 50 h) and following secondary step (shelf temperature 20 °C, chamber pressure 0 mT, 10 h) using Dura-Top™ and Dura-Stop™ freeze-dryer system (FTS Systems, Inc., Stone Ridge, NY). The vials were plugged with nitrogen under reduced pressure and stored under various temperatures (4, 25, and 37 °C). The recovery efficiency and the loading efficiency were calculated as follows.

$$\text{Recovery efficiency}(\%) = \frac{\text{total amount in obtained nanoparticles}}{\text{amount of feed}}$$

$$\text{Loading efficiency}(\text{wt.}\%) = \frac{\text{amount of BP in nanoparticles}}{\text{amount of PLA in nanoparticles}}$$

2.3. Ingredients of a formulation

Seven milliliters of water was added to a vial after lyophilization. The resulting suspension was agitated, after which the volume of the suspension was exactly adjusted at 10 ml by addition of water using a messflask. This suspension was used for each analysis as follows.

2.3.1. BP

The nanoparticles suspension (200 μl) was added to 600 μl of acetonitrile and the solution was agitated to dissolve PLA and PEG-PLA completely. After the addition of 1200 μl of EDTA aqueous solution (50 mM, pH 7.0) to chelate zinc, the BP content in the solution was determined by HPLC (Ishihara et al., 2009a). The content of unencapsulated BP in the suspension was also determined as follows. The nanoparticles suspension was mixed with equal volume of EDTA aqueous solution (50 mM, pH 7.0). After centrifugation of the solution in the filter cap of Ultrafree-MC centrifugal filter unit (Ultrafree-MC with PL-30 membrane, Millipore) at 5000 × g for 30 min, the BP content in the filtrate was determined by HPLC. The residual BP in the nanoparticles was calculated as the difference between total BP and unencapsulated BP.

2.3.2. Acetone and metals

The nanoparticles suspension (1 ml) was added to 1 ml of 6 M sodium hydroxide aqueous solution. After incubation for 3 h at room temperature, 1 ml of 8 M hydrochloric acid aqueous solution was added on ice bath. This acidic solution was used for gas chromatography analysis using GC-2014 (Shimadzu Co., Kyoto, Japan) and Rtx-624 column to determine the acetone content in a vial. The acidic solution was also used for the determination of metals. The zinc and stannous content of the solution was evaluated by Induc-

tively Coupled Plasma Atomic Emission Spectroscopy (ICPS-8000, Shimadzu) (Wendt and Fassel, 1965).

2.3.3. DEA

The nanoparticles suspension (200 μl) was added to 600 μl of acetonitrile. After the addition of 1200 μl of water, the solution was centrifuged at 20,000 × *g* for 30 min at 4 °C. The supernatant was diluted with 2-fold volume of water, after which DEA in the solution was determined by ion chromatography using TSKgel SuperIC-Cation Column (Tosoh Co., Tokyo, Japan).

2.3.4. Citric acid

The nanoparticles suspension (1000 μl) was centrifuged at 39,000 × *g* for 30 min at 4 °C. The supernatant was diluted with 99-fold volume of water, after which citric acid in the solution was determined by ion chromatography using TSKgel OApak-A column (Tosoh).

2.3.5. Sucrose

The nanoparticles suspension (100 μl) in the filter cap of Ultrafree-MC centrifugal filter unit was centrifuged at 5000 × *g* for 30 min at 4 °C. The filtrate was diluted with 2-fold volume of water and then with 9-fold volume of acetonitrile. The mixture was analyzed by HPLC using Asahipak NH2P-50 4E column (Showa Denko K.K. Kawasaki, Japan) and a RI detector, with water/acetonitrile (25/75 v/v) as the mobile phase.

2.3.6. Lactic acid

The nanoparticles suspension was mixed with an equal volume of 4 M sodium hydroxide aqueous solution. After incubation of the suspension for 18 h at 50 °C, 9-fold volume of 340 mM phosphoric acid aqueous solution was added. The content of lactic acid was determined by HPLC using Inertsil ODS-2 column (GL Sciences Inc., Tokyo, Japan) and an UV/vis detector, with 20 mM phosphoric acid aqueous solution as the mobile phase.

2.3.7. Polysorbate 80

In the case of polysorbate 80, 3 ml of methanol-d_4 instead of water was added to a vial. The suspension was allowed at −30 °C for 1 h and then centrifuged at 20,000 × *g* for 3 min at 0 °C. The resulting supernatant was incubated at 50 °C for 2 h and then centrifuged at 20,000 × *g* for 3 min at room temperature. The supernatant was diluted with equal volume of methanol-d_4 containing of 2 mg/ml benzene, after which the solution was analyzed by ^{1}H NMR using JNM-ECP 600 (Jeol Datum Ltd., Tokyo, Japan). Based on the peak area of an internal standard (benzene), the concentration of polysorbate 80 was calculated from peak area in 0.9 ppm derived from oleate.

2.4. Size of nanoparticles

The particle size was determined by the dynamic light scatter method (Zetasizer Nano ZS, Malvern Instruments Ltd, Worcestershire, UK). The nanoparticles suspension was diluted with 4-fold volume of water, after which the size was measured. Also, NIST traceable particle size standard (STADEX 100 nm, 123 nm, 144 nm, JSR Co., Tokyo, Japan) was measured. The size of the nanoparticles was adjusted based on those of the standard particles.

2.5. Release behavior of component of nanoparticles

The nanoparticles with fluorescein were dispersed in the phosphate-buffered saline (PBS) at a BP concentration of 50 μg/ml. After incubation at 37 °C at specified times, the suspension (100 μl) was centrifuged at 39,000 × *g* for 30 min. The precipitate was washed with water by centrifugation and then freeze-dried. The content of lactic acid and BP in the precipitate was determined as reported (Ishihara et al., 2008, 2009a). After dissolution of the dried precipitate in DMF, the fluorescein content was fluorometrically determined using a fluorescence detector (RF-5300PC, Shimadzu) at excitation wavelength 525 nm and emission wavelength 546 nm.

2.6. Animal experiments

Accumulation of the nanoparticles encapsulating fluorescence dye in inflammatory lesion was evaluated by in vivo imaging. Arthritis was induced in Lewis rats (7 weeks old male, weighing 200–250 g, obtained from SLC (Shizuoka, Japan)) by injecting 50 μl of incomplete Freund's adjuvant solution (DIFCO, Detroit, MI) containing 6 mg/ml of *Mycobacterium butyricum* into the subplantar region of the left hind paw (Ishihara et al., 2009c). Five hundred microliters of Cy7-dodecylamine aqueous solution (2.6 μg/ml) or the suspension of nanoparticles encapsulating Cy7-dodecylamine conjugate (Cy7-dodecylamine: 2.6 μg/ml) was intravenously administrated in adjuvant arthritis rats on 14 days after administration of the adjuvant. After 1 day, fluorescence images of left hind paw were observed by explore Optix in vivo fluorescence imaging system (GE Healthcare).

The BP content in the left hind paw was also determined. The nanoparticles with BP (40 μg as BP/500 μl of saline) were intravenously administrated in adjuvant arthritis rats on 14 days after administration of the adjuvant. At specified times, the hind paw was amputated and frozen. The paw was incised using a knife and incubated for 18 h at 37 °C in Hanks' balanced salt solution including 0.05% type 1 collagenase, 0.05% elastase, 0.05% trypsin, 16 U/ml dispase, 0.02% hyaluronidase, 1 mM sodium calcium and 1 mM sodium magnesium. After repeated freeze–thawing (three times), 3-fold volume of acetonitrile and 5.5-fold volume of water were added in this order. The suspension was filtrated through 0.45-μm filter, after which the filtrate was dried using a vacuum concentrator. The dried residue was incubated with alkaline phosphatase (2.7 units/ml, from calf intestine; Toyobo, Tokyo, Japan) and the resulting betamethasone was extracted by ethyl acetate. After dry up of ethyl acetate, betamethasone in the residue was determined by TR-FIA immunoassay. The BP content was shown as weight of detected betamethasone per weight of wet amputated paw.

All animal experiments were performed in accordance with the Animal Experiment Guidelines of the Jikei University School of Medicine.

3. Results and discussion

The nanoparticles were prepared using the PEG-PLA block polymer containing fluorescein at one terminal of the PEG chain. The residual content of BP, lactic acid, and fluorescein in the nanoparticles was determined during incubation in PBS at 37 °C. As shown in Fig. 1A, a large amount of fluorescein was rapidly released from the nanoparticles (residual fluorescein at 4 days, 31%), while BP and lactic acid were gradually released. In a previous study, we analyzed the internalization of various nanoparticles in macrophage-like cells (RAW264.7) after preincubation of the nanoparticles (Ishihara et al., 2009b). The internalization of the nanoparticles (same as described in Fig. 1A) accelerated after a 3-day preincubation period. The results of the previous study along with those of the present study indicate that the release of PEG from the surface of the nanoparticles enhances the affinity of nanoparticles for cells. In addition, the extent of internalization did not depend on the length of the PLA/PLGA segments in the block copolymers but on the composition of PLA/PLGA. This suggests that the release of PEG from the nanoparticles was triggered by the hydrolysis of the PLA/PLGA segment and not by the dissociation of the block copolymers (Ishihara et al., 2009b). In this study, fluorescein released from the nanopar-

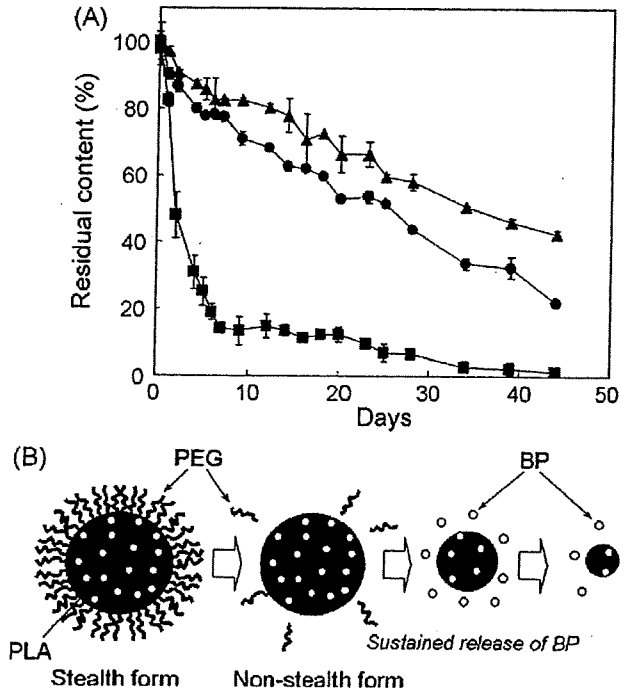

Fig. 1. Degradation of nanoparticles during incubation. (A) Release behavior of each component of the nanoparticles. The amount of BP (circle), lactic acid (triangle), and fluorescein (square) in the nanoparticles was determined during the incubation of nanoparticles in PBS at 37 °C. Each data point represents the mean ± standard deviation (SD) of 3 independent experiments. (B) Schematic illustration of the degradation of nanoparticles during incubation.

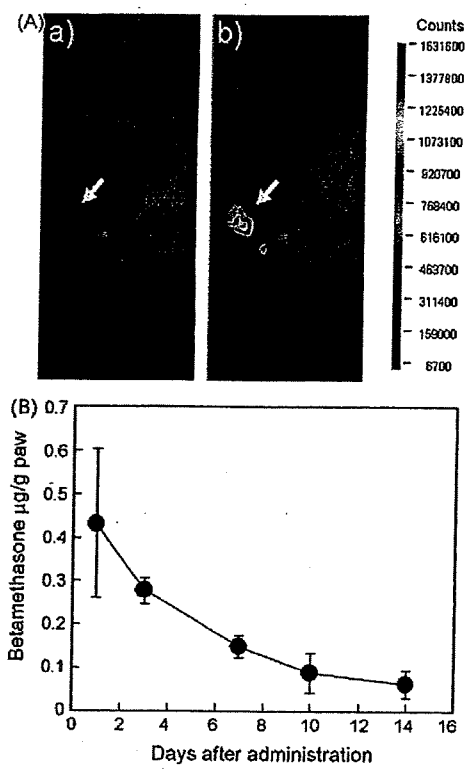

Fig. 2. Accumulation of nanoparticles in the inflammatory lesion in an adjuvant arthritis rat model. (A) Accumulation of (a) Cy7-dodecylamine or (b) Cy7-dodecylamine conjugate-encapsulated nanoparticles on the first day after intravenous administration. The left hind paw of rats was observed using the explore Optix in vivo fluorescence imaging system. The color bar shows the fluorescence intensity (count) of Cy7. (B) The betamethasone content in the inflammatory lesion (left hind paw) was determined as described in Section 2.6 after the administration of the nanoparticles to adjuvant arthritis rat models. Each data point represents the mean ± SD of 3 rats.

ticles into the bulk solution was determined by a fluorometric analysis. In addition, gel permeation chromatography was performed; it revealed that the molecules with fluorescein in the bulk solution had approximately the same molecular weight as a PEG segment, indicating the production of fluorescein-PEG-(lactic acid) [or oligo(lactic acid)] as a result of the hydrolysis of the PLA segment. After alkali-hydrolysis of the nanoparticles, we measured the residual lactic acid content and found that the content gradually decreases during the period of incubation. In addition, the residual BP content corresponded to the residual lactic acid content. This observation suggested that BP is uniformly distributed in the nanoparticles and is released because of surface erosion during PLA hydrolysis (Fig. 1B). The residual content of BP, lactic acid, and fluorescein was measured when the nanoparticles were incubated for 44 days at 4 °C and was found to be 96.1 ± 2.4%, 95.7 ± 1.4%, and 99.9 ± 0.7%, respectively, indicating that the degradation of nanoparticles is greatly inhibited at low temperatures.

A Cy7-dodecylamine conjugate that was used as a labeling material for in vivo imaging was encapsulated in the nanoparticles. Imaging analysis demonstrated preferential accumulation of the nanoparticles in the target lesion (i.e., the left hind paw) (Fig. 2A); this preferential accumulation is probably attributable to the EPR effect. At 1 day after the administration of the nanoparticles, the amount of BP in the lesion was considerably high (Fig. 2B), while after administration of BP alone, the amount of BP was below the detection limit (below 0.04 μg/g tissue). Generally, it is believed that because of the EPR effect, the prolonged residence of carriers in the blood leads to higher accumulation in the lesions. However, higher accumulation does not necessarily correspond to higher therapeutic activity because the local distribution of the carriers in the lesion after circulation remains unknown (Romberg et al., 2008). In a previous study on animals, we found that the nanoparticles with the longest blood half-life did not have the highest anti-inflammatory activity (Ishihara et al., 2009c). The carriers may show stealth properties in the lesion. Such carriers probably have a low affinity for cells and may reenter the blood circulation or a lymph vessel during prolonged residence. On the other hand, depending on the drugs used, it is necessary to determine whether drugs should be released in the intracellular space or the extracellular spaces. In some studies, PEG was formulated such that after its accumulation in the tumor, it would be released from the carriers in response to stimuli such as change in pH and enzymatic reaction, and would thus result in higher therapeutic activity (Mishra et al., 2004; Ambegia et al., 2005; Hatakeyama et al., 2007). Therefore, the stealthiness of the nanoparticles should be controlled in a time-dependent manner to achieve high therapeutic efficiency.

As observed in Fig. 2B, the BP content gradually decreased and was detected even at 14 days after administration. Although we have no apparent evidence to explain this phenomenon, the results obtained in vitro provide a potent hypothesis. The nanoparticles initially possess abundant PEG chains on their surfaces but these are lost within a few days. During this time, most of the BP still remains in the nanoparticles and subsequently is gradually released as shown in Fig. 1A. These results indicated that the accumulation of nanoparticles in the lesion (inflamed paw) was due to the EPR effect and that the internalization of the nanoparticles in inflammatory macrophages was induced by the loss of PEG from the surfaces of the nanoparticles. Thereafter, BP may be gradually released in the cells during PLA hydrolysis. However, the period of residence (approximately 14 days) of BP in the lesion was shorter than that of the release of BP from the nanoparticles in vitro (over 44 days)

Table 1
Ingredients of the freeze-dried formulation.

	Content/vial
BP (mg)	5.6
Betamethasone (μg)	5.6
Acetone (μg)	340
Zinc (μg)	1130
Stannum (μg)	3.0
Diethanolamine (μg)	190
Citric acid (μg)	440
Polysorbate 80 (mg)	3.7
Sucrose (mg)	430
PLA (mg)	40.6

as shown in Figs. 1A and 2A. In a previous report, we showed that during in vitro incubation of cells for 8 days, approximately 80% of the BP in nanoparticles internalized in cells was released from the cells (Ishihara et al., 2005). These results strongly suggested that the release of BP from cells was accelerated because of hydrolysis in an acidic environment such as in endosomes or lysosomes. The release rates of drugs from carriers also significantly influence therapeutic activity.

Stealth nanoparticles with a maximum therapeutic potential should be designed by taking the following two factors into consideration: (i) the time-controlled distribution of drugs in the body or tissue and (ii) the time-controlled release of drugs. The nanoparticles presently used have two time switches: one controls the stealth property, which is observed during the association or dissociation of PEG, and another controls the period of BP release. This simple technique based on the hydrolysis of biodegradable polymers will greatly contribute to the design and optimization of nanoparticles for various applications in a clinical setting.

Next, we attempted to execute the preparation of the nanoparticles on a large-scale in order to evaluate manufacture on an industrial scale. Nanoparticles with the same properties as those that are prepared on a small-scale could be successfully prepared on an 800-fold scale. They were sterilized by filtration using a 0.2-μm membrane filter and freeze-dried in the presence of sucrose. The nanoparticles in the freeze-dried formulation could be uniformly dispersed in water and had the same diameter as nanoparticles that were not subjected to freeze-drying because the sucrose acted as a lyoprotectant and prevented the aggregation of nanoparticles (Ishihara et al., 2005). In this manufacturing process, the recovery efficiency of BP and PLA (i.e., the total amount of PLA in the mixture of PEG-PLA and PLA) was 24.1 wt.% and 26.3 wt.%, respectively. In order to reduce the cost, we need to increase the recovery efficiency of the nanoparticles, because a large amount of the cost depends on that of PEG-PLA and PLA. The loading efficiency of BP in the nanoparticles was 13.8 wt.%. Although it would be ideal to increase the loading efficiency and thus decrease the amount of additives, higher loading may affect the properties of the nanoparticles. In principle, it may be easy to achieve further scale-up because homogenizers or emulsifiers are not used in this method.

The additives used in the manufacture of nanoparticulate formulations seem to be acceptable for clinical use. A number of Food and Drug Administration (FDA)-approved products available in the market contain PLA and PLGA for use as excipients to achieve sustained release of the bioactive molecules (Chaubal, 2002). In addition, block polymers containing PEG and PLA/PLGA also seem to be safe for use because many animal experiments have shown that these polymers are biocompatible and have low immunogenicity and little toxicity (Shive and Anderson, 1997; Plard and Bazile, 1999). Some ongoing clinical trials will, in the near future, clarify the safety of these polymers. In addition to BP, extremely small amounts of betamethasone were also detected by HPLC in the freeze-dried nanoparticles (Table 1). This may be explained by the

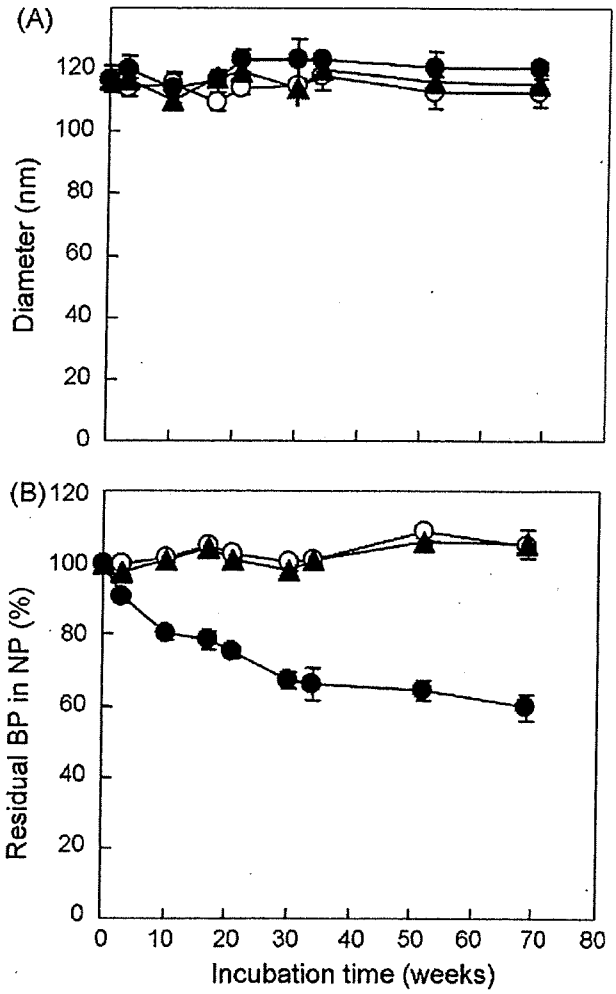

Fig. 3. Storage stability of the freeze-dried nanoparticles at various temperatures (open circle, 4 °C; closed triangle, 25 °C; and closed circle, 37 °C). (A) Diameters of the nanoparticles after resuspension in water. (B) Residual BP content in the nanoparticles. Each data point represents the mean ± SD of 3 independent experiments.

possible production of betamethasone because of the hydrolysis of BP, which occurred during the process of nanoparticle preparation. It is possible to reduce the residual content of acetone to 340 μg per vial by ultrafiltration and freeze-drying (Table 1). According to the Guidelines for Residual Solvents (International Conference on Harmonisation [ICH] Harmonised Tripartite Guidelines), acetone is classified into class 3, and the level of permitted daily exposure (PDE) is limited to <50 mg per day. Hence, the residual content of acetone in the formulation was sufficiently low. Zinc is one of the vital minerals. The level of residual zinc also seems acceptable because zinc chloride solution has been used as an additive in intravenous solutions for total parenteral nutrition (Zinc Chloride Injection, Hospira Inc., Lake Forest, IL). Stannous octoate was used as a catalyst for the polymerization of PLA/PLGA. Since this compound is accepted by the FDA as a food additive (Kim et al., 1992) and the level of stannum in the formulation was extremely low (3 μg per vial, Table 1), the residual stannum content is acceptable as discussed elsewhere (Gunatillake and Adhikari, 2003). Further, other materials used in the formulation that are listed in Table 1 have already been used as additives in a clinical setting.

We evaluated the stability of freeze-dried nanoparticles during storage at various temperatures. The diameters of the nanoparticles were constant even after resuspension in water (Fig. 3A) and

no chemical changes in BP were observed on varying the temperature (data not shown). On the other hand, we did not observe leakage (release) of BP from the freeze-dried nanoparticles during 69 weeks of incubation at 4 °C and 25 °C, while BP was released during incubation at 37 °C (Fig. 3B). This temperature-dependent release may be attributable to the thermodynamic stability of the polymers (PLA and PEG-PLA) used in the nanoparticle preparation. In general, the glass transition temperature (T_g) of a polymer is the temperature at which the polymer changes from the glassy state to the rubbery state. In the rubbery state, the diffusion of the drug from the nanoparticles is easier because of the high mobility of the polymer chains (Wischke and Schwendeman, 2008). On the basis of this finding, we can conclude that this formulation can be stably stored at low temperatures (below 25 °C) for at least 69 weeks.

4. Conclusions

Polymeric nanoparticles formed using a blend of PLA and PEG-PLA with BP were prepared by an oil-in-water solvent diffusion method. The results of the present and previous studies have strongly suggested the behavior of the nanoparticles in vivo: initial accumulation in the lesion, internalization in inflammatory macrophages, and gradual release of BP in cells. Furthermore, the nanoparticles were successfully prepared on a large-scale, and freeze-dried nanoparticles were stably stored for at least 69 weeks below 25 °C. The present results indicate that this nanoparticulate formulation can be used in a clinical setting.

Acknowledgements

The authors thank Dr. Eri Ayano, Tetsushi Kubota, Sachiyo Shibata, Emi Shimada, and Sachiko Seki for their helpful advices and technical assistance with the experiments. The authors also thank Shionogi & Co., Ltd. for supplying the TR-FIA assay kit.

References

Ambegia, E., Ansell, S., Cullis, P., Heyes, J., Palmer, L., MacLachlan, I., 2005. Stabilized plasmid–lipid particles containing PEG-diacylglycerols exhibit extended circulation lifetimes and tumor selective gene expression. Biochim. Biophys. Acta 1669, 155–163.

Chaubal, M., 2002. Polylactides/glycolides—excipients for injectable drug. Drug Deliv. Technol. 2, 34–36.

Gunatillake, P.A., Adhikari, R., 2003. Biodegradable synthetic polymers for tissue engineering. Eur. Cell Mater. 5, 1–16.

Hatakeyama, H., Akita, H., Kogure, K., Oishi, M., Nagasaki, Y., Kihira, Y., Ueno, M., Kobayashi, H., Kikuchi, H., Harashima, H., 2007. Development of a novel systemic gene delivery system for cancer therapy with a tumor-specific cleavable PEG–lipid. Gene Ther. 14, 68–77.

Ishihara, T., Izumo, N., Higaki, M., Shimada, E., Hagi, T., Mine, L., Ogawa, Y., Mizushima, Y., 2005. Role of zinc in formulation of PLGA/PLA nanoparticles encapsulating betamethasone phosphate and its release profile. J. Control. Release 105, 68–76.

Ishihara, T., Takahashi, M., Higaki, M., Takenaga, M., Mizushima, T., Mizushima, Y., 2008. Prolonging the in vivo residence time of prostaglandin E1 with biodegradable nanoparticles. Pharm. Res. 25, 1686–1695.

Ishihara, T., Takahashi, M., Higaki, M., Mizushima, Y., 2009a. Efficient encapsulation of a water-soluble corticosteroid in biodegradable nanoparticles. Int. J. Pharm. 365, 200–205.

Ishihara, T., Kubota, T., Choi, T., Takahashi, M., Ayano, E., Kanazawa, H., Higaki, M., 2009b. Polymeric nanoparticles encapsulating betamethasone phosphate with different release profiles and stealthiness. Int. J. Pharm. 375, 148–154.

Ishihara, T., Kubota, T., Choi, T., Higaki, M., 2009c. Treatment of experimental arthritis with stealth-type polymeric nanoparticles encapsulating betamethasone phosphate. J. Pharm. Exp. Ther. 329, 412–417.

Kim, S.Y., Han, Y.K., Kim, Y.K., Hong, S.I., 1992. Multifunctional initiation of lactide polymerization by stannous octoate/pentaerythritol. Makromol. Chem. 193, 1623–1631.

Maeda, H., Wu, J., Sawa, T., Matsumura, Y., Hori, K., 2000. Tumor vascular permeability and the EPR effect in macromolecular therapeutics: a review. J. Control. Release 65, 271–284.

Mishra, S., Webster, P., Davis, M.E., 2004. PEGylation significantly affects cellular uptake and intracellular trafficking of non-viral gene delivery particles. Eur. J. Cell Biol. 83, 97–111.

Moghimi, S.M., Hunter, A.C., Murray, J.C., 2001. Long-circulating and target-specific nanoparticles: theory to practice. Pharm. Res. 53, 283–318.

Peer, D., Karp, J.M., Hong, S., Farokhzad, O.C., Margalit, R., Langer, R., 2007. Nanocarriers as an emerging platform for cancer therapy. Nat. Nanotechnol. 2, 751–760.

Plard, J.P., Bazile, D., 1999. Comparison of the safety profiles of PLA50 and Me.PEG-PLA50 nanoparticles after single dose intravenous administration to rat. Colloids Surf. B: Biointerfaces 16, 173–183.

Riley, T., Stolnik, S., Heald, C.R., Xiong, C.D., Garnett, M.C., Illum, L., Davis, S.S., 2001. Physicochemical evaluation of nanoparticles assembled from poly(lactic acid)-poly(ethylene glycol) (PLA-PEG) block copolymers as drug delivery vehicles. Langmuir 17, 3168–3174.

Romberg, B., Hennink, W.E., Storm, G., 2008. Sheddable coatings for long-circulating nanoparticles. Pharm. Res. 25, 55–71.

Shive, M.S., Anderson, J.M., 1997. Biodegradation and biocompatibility of PLA and PLGA microspheres. Adv. Drug Deliv. Rev. 28, 5–24.

Wendt, R.H., Fassel, V.A., 1965. Induction-coupled plasma spectrometric excitation source. Anal. Chem. 37, 920–922.

Wischke, C., Schwendeman, S.P., 2008. Principles of encapsulating hydrophobic drugs in PLA/PLGA microparticles. Int. J. Pharm. 364, 298–327.

Yih, T.C., Al-Fandi, M., 2006. Engineered nanoparticles as precise drug delivery systems. J. Cell. Biochem. 97, 1184–1190.

HSP-Dependent Protection Against Gastrointestinal Diseases

Tohru Mizushima*

Graduate School of Medical and Pharmaceutical Sciences, Kumamoto University, Kumamoto 862-0973, Japan

Abstract: It is well known that heat shock proteins (HSPs) are induced by various stressors in order to confer protection against such stressors. Since stressor-induced tissue damage is involved in various diseases, especially gastrointestinal diseases, such as gastric ulcer, it has been thought that HSPs are protective against these diseases. Indirect lines of evidence, such as identification of geranylgeranylacetone (GGA, a leading anti-ulcer drug in Japanese market) as non-toxic HSP-inducer, suggest that HSPs provide a major protective mechanism against irritant-induced gastric lesions. However, no direct evidences that support this notion exits. Furthermore, because GGA has other gastroprotective effects, it was not clear whether HSP-induction by GGA is the main mechanism for its anti-ulcer effect. In this article, I review our recent work on protective roles of HSPs against gastrointestinal diseases, using transgenic mice. We obtained genetic evidence showing not only that HSPs are protective against irritant-induced gastric lesions but also that GGA achieves its anti-ulcer effect through induction of HSPs. We also obtained genetic evidence that HSPs are protective against inflammatory bowel disease (IBD)-related colitis and lesions of small intestine. Furthermore, we found that GGA is effective against these diseases. Based on these observations, we propose that non-toxic HSP-inducers, such as GGA are therapeutically beneficial for these diseases.

Keywords: HSP70, HSF1, gastric ulcer, IBD, lesions of the small intestine, GGA.

BACKGROUNDS FOR HSPs

When cells are exposed to stressors, a number of so-called stress proteins are induced, in order to confer protection against such stressors. Heat shock proteins (HSPs) are representative of these stress proteins, and their cellular up-regulation, especially that of HSP70, provides resistance as they re-fold or degrade denatured proteins produced by the stressors [1]. It has been reported not only that various stressors up-regulate HSPs, but also that artificial up-regulation of HSPs confers resistance to these stressors in cultured cells [1]. The up-regulation of HSPs by various stressors is regulated at the transcription level by a consensus *cis*-element (heat shock element (HSE)) and a transcription factor (heat shock factor 1 (HSF1)), that specifically binds to HSE located on the upstream region of *hsp* genes [2].

Since cytoprotective effect of HSPs is potent and cell death (tissue damage) by stressors play an important role in pathogenesis of various types of diseases, HSPs have been thought to be interesting target of drugs, however, non-specificity of HSPs (induction by various stressors and protection of cells against various stressors) is a obstacle for such drug development (it is generally believed that drug should be specific). However, I consider that this non-specificity of HSPs is of advantage for some type of gastrointestinal diseases, such as gastric ulcers, because development of these diseases is triggered by cell damage induced by various irritants and thus, drugs that non-specifically protect cells against irritants may be beneficial for these diseases.

Supporting this notion, geranylgeranylacetone (GGA), a leading anti-ulcer drug on the Japanese market, has been reported to be a non-toxic HSP-inducer, up-regulating various HSPs not only in cultured gastric mucosal cells at concentrations that do not affect cell viability but also in various tissues, including the gastric mucosa *in vivo* [3, 4]. We have previously reported that pre-induction of HSPs by GGA protects cultured gastric mucosal cells from cell death induced by various irritants [5-8]. These previous results suggest that the anti-ulcer effect of GGA is due to its HSP-inducing activity.

*Address correspondence to this author at the Graduate School of Medical and Pharmaceutical Sciences, Kumamoto University, 5-1 Oe-honmachi, Kumamoto 862-0973, Japan; Tel/Fax: 81-96-371-4323;
E-mail: mizu@gpo.kumamoto-u.ac.jp

PROTECTIVE EFFECT OF HSPs AGAINST IRRITANT-INDUCED GASTRIC LESIONS

The balance between aggressive and defensive factors determines development of gastric lesions. The gastric mucosa is challenged by a variety of both endogenous and exogenous irritants (aggressive factors), including ethanol, gastric acid, pepsin, non-steroidal anti-inflammatory drugs (NSAIDs) and *Helicobacter pylori*. These irritants damage the mucosal cells, inducing cell death which leads to the formation of gastric lesions [9]. In order to protect the gastric mucosa, a complex defence system, which includes the production of surface mucus and bicarbonate and the regulation of gastric mucosal blood flow has evolved. Prostaglandins (PGs), in particular PGE_2, enhance these protective mechanisms, and are therefore thought to comprise a major gastric mucosal defensive factor [10].

Recently, HSPs have attracted considerable attention as another major defensive factor for gastric mucosa. However, very little direct evidence exists. As for GGA, because GGA mediates various other gastro-protective mechanisms [11, 12], it remains unclear whether up-regulation of HSPs represents GGA's major mode of anti-ulcer activity. To address these issues, we used HSF1-null mice and transgenic mice expressing HSP70 to obtain direct genetic evidence for the contribution of HSPs to the protection of the gastric mucosa and to GGA's major mode of anti-ulcer activity.

As shown in Fig. **(1A)**, intragastric administration of indomethacin resulted in production of higher level of gastric lesions in HSF1-null mice than in wild-type mice. Similar results were obtained with ethanol and hydrochloric acid-induced gastric lesions [13, 14]. Given that HSF1 up-regulates the expression of HSPs, we examined the effect of indomethacin administration on the mRNA expression of HSPs in the gastric mucosa of HSF1-null mice and wild-type mice. Indomethacin administration up-regulated the mRNA expression of only HSP70, a response that was dependent on the function of HSF1 [14]. Based on these results, we subsequently focused on HSP70.

The level of indomethacin-induced gastric lesions was compared between transgenic mice expressing HSP70 and wild-type mice. Relative to control mice, formation of indomethacin-induced gastric lesions was significantly suppressed in transgenic mice expressing HSP70 Fig. **(1B)**. By immunoblotting and immuno-histochemical analyses, we confirmed that HSP70 expression

1381-6128/10 $55.00+.00

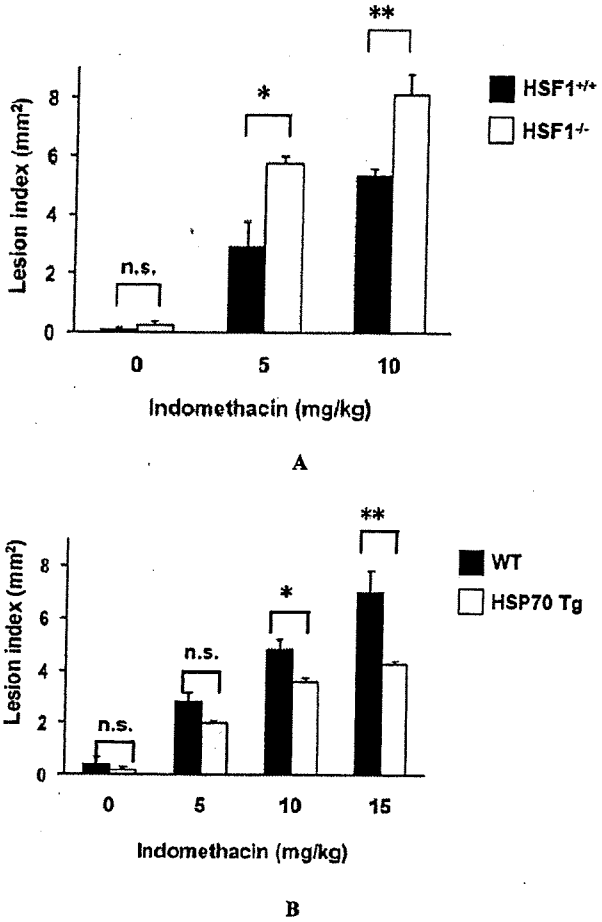

Fig. (1). Production of gastric lesions by indomethacin. HSF1-null mice (-/-) and wild-type mice (+/+) (**A**) or transgenic mice expressing HSP70 (HSP70 Tg) and wild-type mice (WT) (**B**) were orally administered the indicated doses of indomethacin and their stomachs were removed after 8 h. The stomach was scored for hemorrhagic damage. Values are mean ± S.E.M. (n = 3-6). $^{**}P<0.01$; $^{*}P<0.05$; n.s., not significant. This figures was published previously and is reprinted here with permission of the journal [14].

was much higher in the gastric tissues of the transgenic mice than in those of the wild-type mice, regardless of whether or not they were treated with indomethacin [14]. These results offer direct genetic evidence that expression of HSP70 protects the gastric mucosa against the formation of irritant-induced gastric lesions. HSP70 normally has a reasonable level of expression in cells and this may contribute to protection of gastric mucosa.

Another group suggested the protective role of HSP27 against indomethacin-induced gastric lesions. Ebert *et al.* reported that transgenic mice expressing HSP27 showed resistant phenotype to indomethacin-induced gastric lesions. They also showed that overexpression of HSP27 did not affect the expression of COX-1 and COX-2, suggesting that expression of HSP27 protects gastric mucosa against NSAID-induced lesions through cytoprotection rather than modulation of inhibition of COX by NSAIDs [15].

In order to investigate the mechanism governing the suppression of production of indomethacin-stimulated gastric lesions in transgenic mice expressing HSP70, we compared the level of apoptosis. In wild-type mice, an increase in TUNEL-positive (apoptotic) cells was observed following the administration of indomethacin, which is suppressed in transgenic mice expressing HSP70 [14]. On the other hand, there was no significant difference in the gastric level of PGE_2 between transgenic mice expressing HSP70 and wild-type mice [14]. These results suggest that HSP70 protects gastric mucosa from NSAID-induced lesions through inhibiting apoptosis rather than affecting gastric PGE_2 levels. Similar results were observed for ethanol-induced gastric lesions [13].

In order to evaluate the contribution of the HSP-inducing activity of GGA to its anti-ulcer activity, we investigated the effect of GGA in HSF1-null mice. If anti-ulcer activity of GGA is mediated by its HSP-inducing activity, GGA would not show the anti-ulcer activity in HSF1-null mice where induction of HSPs is suppressed. First, we examined the effect of GGA and/or indomethacin on gastric mucosal HSP70 expression in wild-type mice, revealing a potent expression induced by indomethacin or GGA in wild-type mice Figs. (**2A** and **B**). Interestingly, pre-administration of GGA enhanced the indomethacin-dependent HSP70 response in wild-type mice Figs. (**2A** and **B**). We confirmed that administration of GGA and/or indomethacin did not induce HSP70 in HSF1-null mice Figs. (**2A** and **B**). Fig. (**2C**) shows the effect of pre-administration of GGA on indomethacin-produced gastric lesions in wild-type and HSF1-null mice. Pre-administration of GGA significantly suppressed the indomethacin-dependent production of gastric lesions in wild-type mice Fig. (**2C**). In contrast, no significant effect was recorded in the HSF1-null mice "Fig. (**2C**)". This result shows that HSF1 is required for the efficacy of the anti-ulcer activity of GGA against indomethacin. Overall, the results in Fig. 2 suggest that the loss of the protective effect of GGA in HSF1-null mice is due to the lack of expression of HSPs (such as HSP70), in other words, the HSP-inducing activity of GGA contributes to its anti-ulcer activity. Similar results were observed for ethanol-induced gastric lesions [13]. These results provide the first direct genetic link between the pharmacological behaviour of the drug and the resultant clinical outcome.

PROTECTIVE EFFECT OF HSPs AGAINST INFLAMMATORY BOWEL DISEASE (IBD)

IBD, Crohn's disease (CD) and ulcerative colitis (UC), have become substantial health problems with an actual prevalence of 200-500 per 100,-000 people in western countries, which almost doubles every 10 years [16]. Although the etiology of IBD is not yet fully understood, recent studies suggest that IBD involves chronic inflammatory disorders in the intestine due to "a vicious cycle". Infiltration of leukocytes into intestinal tissues cause intestinal mucosal damage induced by reactive oxygen species (ROS) that are released from the activated leukocytes, and this intestinal mucosal damage further stimulates the infiltration of leukocytes [17]. To understand the molecular mechanism underlying the pathogenesis of IBD and to develop new types of clinical drugs for IBD, identification of endogenous factors that positively or negatively affect the development of IBD is important. For this purpose, various experimental animal colitis models, in particular the dextran sulfate sodium (DSS)-induced colitis models, have been used [18]. Pro-inflammatory cytokines and cell adhesion molecules (CAMs) play an important role in the activation and infiltration of leukocytes that is associated with IBD [19, 20].

HSPs and HSF1 also have attracted considerable attention as candidates for endogenous factors that affect the development of IBD because some HSPs, including HSP70, were reported to be over-expressed in the intestinal tissues of IBD patients and in an animal model of IBD [21]. HSF1 negatively regulates the expression of tumor necrosis factor (TNF)-a and interleukin (IL)-1b [22]. These previous results suggest that HSPs and HSF1 have negative roles on the development of IBD, however, there is no direct evidence (such as genetic evidence) to support this idea. Furthermore, there are some data that suggest positive roles for HSPs and HSF1 in the development of IBD [23]. Therefore, the

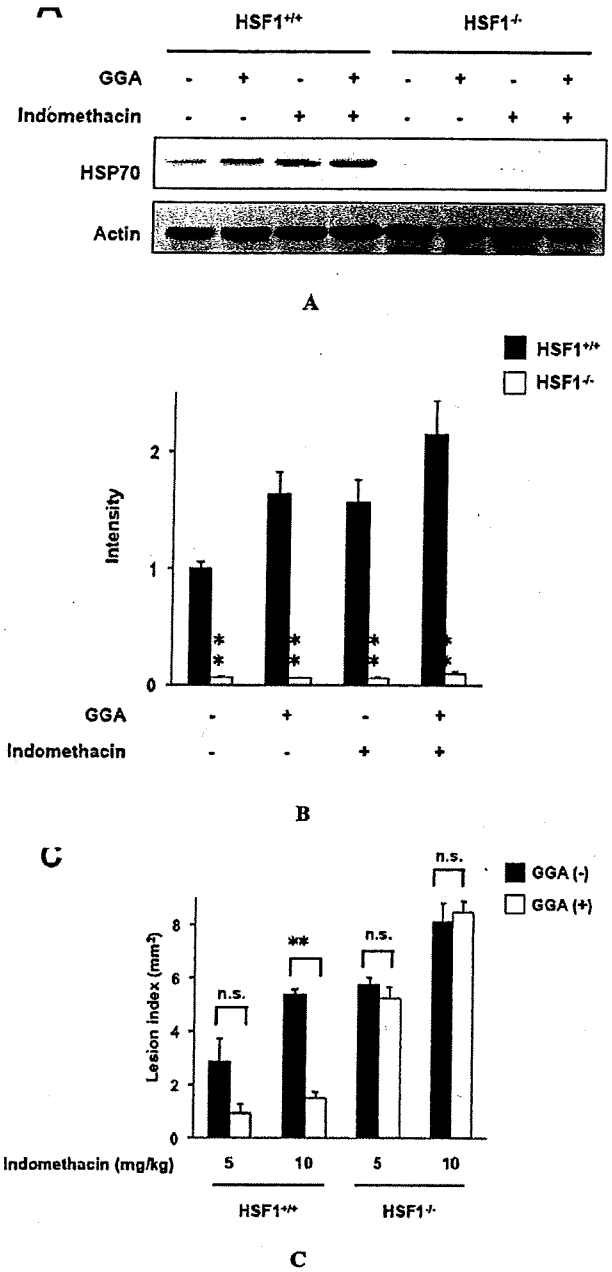

Fig. (2). Effect of indomethacin and/or GGA on expression of HSP70 and production of gastric lesions. HSF1-null mice (-/-) and wild-type mice (+/+) were orally administered 50 mg/kg GGA, 1 h after which they were orally administered 10 mg/kg (A, B) or the indicated doses (C) of indomethacin and the stomach was removed after 8 h. A, immunoblotting analyses were performed. B, experiments shown in C were repeated for six mice per one condition and the results (band intensity of HSP70) were analysed statistically. Values are mean ± S.E.M. (n = 6). **P<0.01. C, gastric mucosal lesions were measured. Values are mean ± S.E.M. (n = 3-4). **P<0.01; n.s., not significant. This figures was published previously and is reprinted here with permission of the journal [14].

effects of genetic alteration of HSPs and HSF1 on the development of colitis in animal models of IBD should be examined in order to understand the exact role (positive or negative) of HSPs and HSF1 in IBD. Thus, we examined the role of HSF1 and HSPs in the pathogenesis of DSS-induced colitis by use of transgenic mice.

The severity of DSS-induced colitis can be monitored by various indexes, such as DAI, length of colon and MPO activity. Administration of 3% DSS caused a mild increase in the DAI and this administration resulted in a higher DAI score in HSF1-null mice Fig. (**3A**). DSS-induced colon shortening, used as a morphometric measure for the degree of inflammation, was more severe in HSF1-null mice than in the wild-type mice [24]. Colonic MPO activity, an indicator of infiltration of leukocytes, was much higher in DSS-administered HSF1-null mice than the wild-type mice [24]. The results show that HSF1-null mice are more sensitive to DSS-induced colitis than their respective wild-type mice. Next, development of DSS-induced colitis was compared in transgenic mice expressing HSP70 and their respective wild-type mice. DSS-dependent increase in DAI was clearly suppressed in transgenic mice expressing HSP70 compared to the wild-type mice Fig. (**3B**). All of the other indexes of colitis that were tested (colon length and colonic MPO activity) showed that transgenic mice expressing

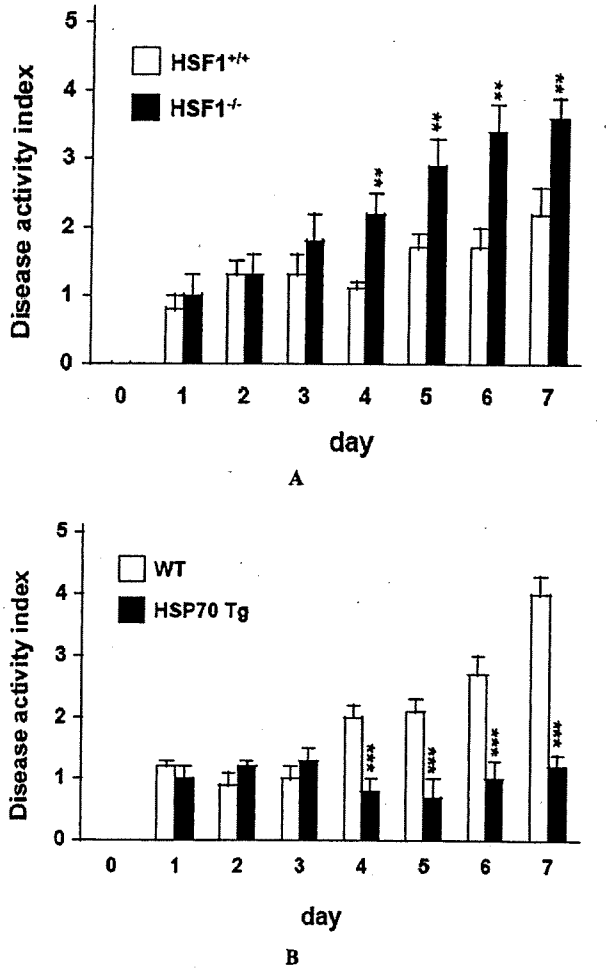

Fig. (3). Development of DSS-induced colitis. HSF1-null mice (-/-) and wild-type mice (+/+) (A) or transgenic mice expressing HSP70 (HSP70 Tg) and wild-type mice (WT) (B) were treated with or without 3% DSS for 7 days. DAI were measured daily. Values are mean ± S.E.M. (n=3-10). ***P<0.01; **P<0.01. n.s. not significant. This figures was published previously and is reprinted here with permission of the journal [24].

HSP70 are more resistant than the wild-type mice to DSS-induced colitis [24].

Another group addressed this issue by use of GGA. Ohkawara *et al.* reported that oral administration of GGA (300-500 mg/kg) suppressed DSS-induced increase in DAI, colon shortening, increase in colonic MPO activity and colonic mucosal damage. They also showed that administration of GGA lowered the colonic level of pro-inflammatory cytokines. Furthermore, they showed that GGA up-regulated the expression of HSP70 and HSP40 but not other HSPs in the colons [25]. They also examined the effect of GGA on trinitrobenzene sulfonic acid-induced colitis, another animal model of IBD. Oral administration of GGA (300 mg/kg) suppressed TNBS-induced decrease in body weight, increase in DAI, increase in colonic MPO activity and colonic mucosal damage. They also showed that the survival rate of mice treated with TNBS significantly increased by GGA administration [26]. These results support the idea that HSPs are protective against IBD-related colitis and suggest that non-toxic inducers of HSP expression are therapeutically beneficial for IBD.

In order to understand the mechanism governing the decreased susceptibility of transgenic mice expressing HSP70 to DSS-induced colitis, we compared the mRNA expression of various inflammation-related proteins in the colonic tissues. The mRNA expression of *tnf*-a, *il-1b* and *il-6* in colonic tissues was significantly lower in DSS-administered transgenic mice expressing HSP70 than in the wild-type mice, suggesting that HSP70 negatively regulate the expression of the selected pro-inflammatory cytokines under inflammatory conditions [24]. To test this idea *in vitro*, we compared the LPS-stimulated production of the pro-inflammatory cytokines (TNF-a, IL-1b and IL-6) in peritoneal macrophages prepared from the transgenic mice and their wild-type counterparts. LPS stimulated the production of all of these pro-inflammatory cytokines and the levels were much lower in the medium of the LPS-treated macrophages prepared from transgenic mice expressing HSP70 than from wild-type mice [24]. These results suggest that expression of HSP70 may suppress the production of these pro-inflammatory cytokines under inflammatory conditions. We speculate that this suppression is mediated by HSP70-dependent inhibition of nuclear factor kappa B (NF-kB), which plays an important role in the induction of inflammation. It is known that NF-kB positively regulates expression of pro-inflammatory cytokines including TNF-a, IL-1b and IL-6. Furthermore, it is also known that up-regulation of HSP70 expression by heat shock inhibits the inflammatory stimuli-dependent activation of NF-kB through various mechanisms [27-33].

We compared mRNA expression of *vcam-1* and *icam-1* in the colonic tissues of transgenic mice and wild-type mice. The mRNA expression of these CAMs was much lower and higher in the DSS-administered transgenic mice expressing HSP70 or HSF-null mice, respectively, than the wild-type mice [24]. *In vitro*, we examined the effect of siRNA specific for HSF1 or HSP70 on the LPS-induced mRNA expression of the CAMs. Transfection with HSF1 siRNA up-regulated the mRNA expression of *vcam-1* and *icam-1* in the presence of LPS. Transfection of the cells with siRNA specific for HSP70 did not significantly up-regulate the mRNA expression of the CAMs in the presence of LPS, suggesting that, at least *in vitro*, HSP70 does not negatively regulate the mRNA expression of these CAMs under inflammatory conditions and HSF1 directly (not through up-regulation of expression of HSP70) suppresses mRNA expression of the CAMs [24].

We compared the level of cell death in the colonic mucosa of DSS-administered transgenic mice expressing HSP70 and the respective wild-type mice by use of the TUNEL assay. Less TUNEL-positive cells were observed in the colonic mucosa of DSS-administered transgenic mice expressing HSP70 than the wild-type mice. The results suggest that ROS-induced cell death associated with DSS-induced colitis is suppressed in transgenic mice expressing HSP70 [24].

To test the role of HSP70 in ROS-induced cell death *in vitro*, we examined the effect of siRNA specific for HSP70 on cell death induced by menadione, a superoxide anion (a representative ROS) releasing drug. Transfection of cells with siRNA for HSP70 clearly stimulated cell death induced by menadione [24]. The results suggest that HSP70 protects colonic cells from ROS-induced cell death and that this effect may be involved in the improved resistance to DSS-induced colitis that is observed in transgenic mice expressing HSP70.

We have gathered evidence that HSF1 and HSPs have negative roles in the development of IBD by demonstrating the sensitive phenotype of HSF1-null mice and the resistant phenotype of transgenic mice expressing HSP70 against DSS-induced colitis.

PROTECTIVE EFFECT OF HSPs AGAINST LESIONS OF THE SMALL INTESTINE

More attention has generally been paid to NSAID-induced gastric lesions rather than lesions of the small intestine, because the latter are usually asymptomatic and their diagnosis was difficult to make. However, recent improvements in the capabilities of diagnostic techniques such as capsule endoscopy and double-balloon endoscopy, have revealed that NSAID-induced lesions of the small intestine occur very frequently and that the small intestine is even more susceptible than gastric tissue to the detrimental effects of NSAIDs [34, 35]. For example, it was reported that 50-70% of chronic users of NSAIDs have lesions of the small intestine [36, 37]. For gastric lesions, COX-2 selective NSAIDs have been developed as safer alternatives; however, animal and clinical studies have revealed that the safety of long-term use of such COX-2 selective NSAIDs with respect to the small intestine is indistinguishable from that of non-selective NSAIDs [34, 38].

Compared to gastric lesions, the etiology of NSAID-induced lesions of the small intestine is not clear at present, thus complicating the establishment of clinical protocols for their treatment. However, recent studies suggest that NSAID-induced lesions of the small intestine share some but not all of the aggressive factors evident with gastric lesions. The direct cytotoxicity (topical effect) of NSAIDs seems to be involved in NSAID-induced lesions of the small intestine [39, 40]. Inflammatory responses, such as the infiltration of neutrophils, stimulate NSAID-induced lesions of the small intestine [41]. Bacterial invasion, bacterial products, bile and nitric oxide (NO) produced by inducible NO synthase (iNOS) also seem to damage the small intestinal mucosa to produce lesions [42-44]. On the other hand, acid secretion is not as important in the development of NSAID-induced lesions of the small intestine. Thus, acid control drugs are not as effective for treating NSAID-induced lesions of the small intestine compared to their effect on gastric lesions [45, 46].

It is reasonable to speculate that HSP70 protects against NSAID-induced lesions of the small intestine, thereby acting as a defensive factor in the small intestine as it does in the case of stomach tissue. While the results of a number of *in vitro* studies support this idea [47], no direct evidence currently exists. Thus, we examined indomethacin-induced lesions of the small intestine in transgenic mice expressing HSP70. Furthermore, we examined the effect of oral administration of GGA on lesions of this type.

The severity of indomethacin-induced lesions in the small intestine was monitored by measurement of a lesion index. We compared between transgenic mice expressing HSP70 and wild-type mice the development of lesions in the small intestine after administration of indomethacin. Indomethacin induced lesions in the small intestine in a dose-dependent manner in wild-type mice and this production was significantly reduced in transgenic mice expressing HSP70 [48]. These results show that transgenic mice

expressing HSP70 are more resistant than wild-type mice to indomethacin-induced lesions of the small intestine.

As described above, a decrease in the level of PGE_2 (COX-inhibition), the presence of mucosal cell apoptosis, and induction of cytokines and chemokines all play important roles in the NSAID-induced production of lesions of the small intestine. We therefore compared these factors between transgenic mice expressing HSP70 and wild-type mice. There was no significant difference in the small intestinal level of PGE_2 between transgenic mice expressing HSP70 and wild-type mice either with or without indomethacin treatment [48]. An increase in the number of TUNEL-positive (apoptotic) cells in the small intestine of wild-type mice was observed after indomethacin administration, and this increase was clearly suppressed in transgenic mice expressing HSP70 [48]. These results suggest that expression of HSP70 protects the small intestine mucosa from lesions by inhibiting indomethacin-induced apoptosis rather than by affecting the level of PGE_2 in the small intestine. The mRNA expression levels of all of cytokines (*il-1b*, *il-6* and *tnf*-a) and chemokines (*mcp-1* and *mip-2*) tested were up-regulated in wild-type mice by the administration of indomethacin. However, the expression of *il-1b*, *il-6* and *mip-2* mRNA was significantly lower in indomethacin-treated transgenic mice expressing HSP70 than in wild-type controls [48]. These results suggest that the reduced expression of these pro-inflammatory cytokines and chemokines in transgenic mice expressing HSP70 is involved in their phenotypic resistance to indomethacin-induced lesions of the small intestine.

We next examined the effect of pre-administration of GGA on indomethacin-induced lesions in the small intestine. As shown in Fig. (**4A**), pre-administration of GGA suppressed the indomethacin-induced lesions in a dose-dependent manner. We also examined the effect of pre-administration of GGA on the indomethacin-dependent decrease in the level of PGE_2 and increased level of mucosal cell apoptosis in the small intestine and found that GGA did not affect this level in the presence of indomethacin but suppressed indomethacin-induced increase in the number of TUNEL-positive cells [48]. These results suggest that the GGA-induced expression of HSP70 suppressed the extent of indomethacin-induced lesions by inhibiting indomethacin-induced mucosal cell apoptosis.

We also examined by immunoblotting analysis the effect of GGA and/or indomethacin on the expression of HSP70 in the small intestine. Administration of indomethacin increased the expression of HSP70 Figs. (**4B** and **4C**), while GGA significantly stimulated the expression of HSP70 in both the presence and absence of indomethacin treatment (Fig. 4B and C). To test the involvement of HSP70 in the protective role of GGA against indomethacin-induced lesions of the small intestine, we examined the effect of pre-administration of quercetin (an inhibitor of expression of HSP70) on the protective effect of GGA. Pre-administration of quercetin diminished the protective effect of GGA against indomethacin-induced lesions of the small intestine, suggesting that GGA suppresses the extent of indomethacin-induced lesions in the small intestine by inducing HSP70 [48].

Gastro-protective drugs, such as GGA, have been used in the treatment of gastric lesions for a long period. However, it is believed that newly developed acid-control drugs (such as H_2-blockers and PPIs) are superior to these gastro-protective drugs in curing/preventing gastric lesions. On the other hand, these acid-control drugs seem to be ineffective against NSAID-induced lesions of the small intestine. Results described above strongly suggest that oral administration of GGA could also be therapeutically beneficial against NSAID-induced lesions of the small intestine in humans owing to its HSP-inducing activity.

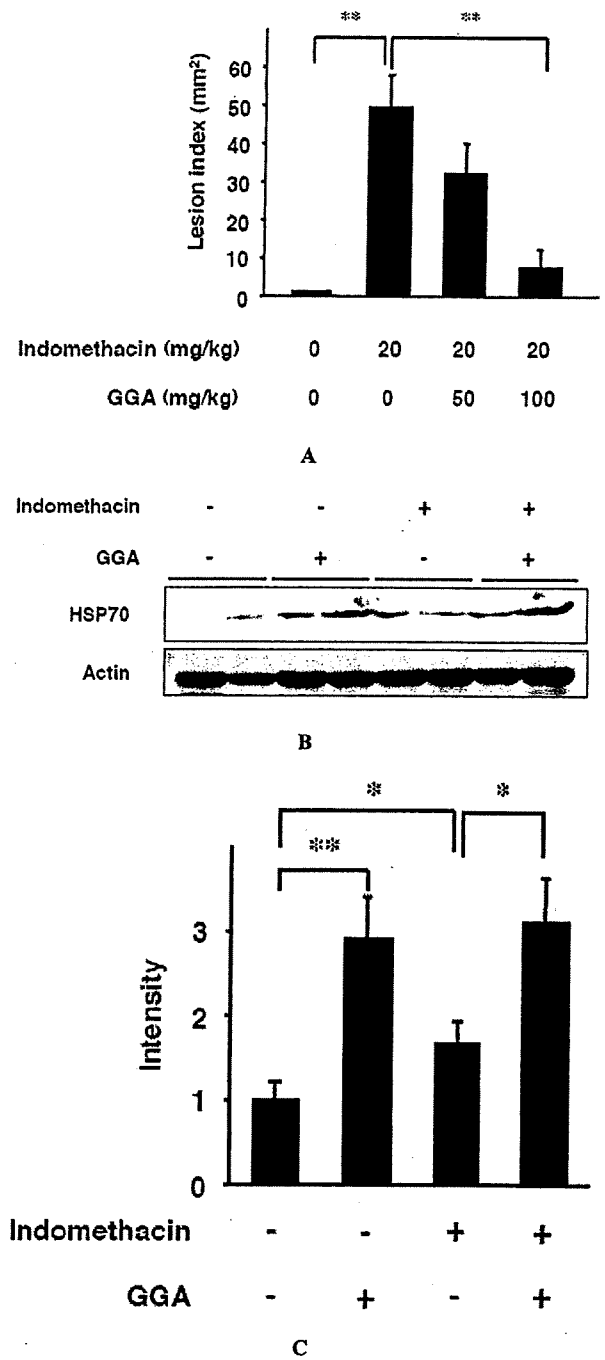

Fig. (4). Effect of GGA on expression of HSP70 and production of lesions in the small intestine. Wild-type mice were orally administered indicated doses (A) or 100 mg/kg (B, C) of GGA Two hours later the mice were orally administered 20 mg/kg of indomethacin. Small intestine was removed 24 h (A) or 4 h (B, C) after the administration of indomethacin. The small intestine was scored for hemorrhagic damage (A). Protein extract was prepared and analysed by immunoblotting with an antibody against HSP70 or actin (B). The band intensity of HSP70 was determined by densitometric scanning, normalized with respect to actin (C). Values are mean ± S.E.M. (n = 3-9 (A), 10-16 (C). $^{**}P<0.01$; $^{*}P<0.05$; n.s., not significant. This figures was published previously and is reprinted here with permission of the journal [48].

CONCLUSION

Analysis of animal model of gastrointestinal diseases in HSF1-null mice and transgenic mice expressing HSP70 is effective for understanding the role of HSPs in these diseases. Our results strongly suggest that HSP70 is protective against irritant-induced gastric lesions, IBD and lesions of the small intestine. Such analysis also showed that the HSP-inducing activity of GGA contributes to its anti-ulcer activity. We also found that GGA is effective for DSS-induced colitis and NSAID-induced lesions of the small intestine. For IBD and lesions of the small intestine, clinical protocol for their treatment has not been established and the development of new molecules as candidate drugs to treat these diseases must pass through the clinical trials process and may encounter the anticipated side effects. Thus, based on our results, we propose that clinical studies should be performed to prove the effectiveness of GGA for treating IBD and NSAID-induced lesions of the small intestine given that the safety of GGA has already been shown clinically.

ACKNOWLEDGEMENTS

This work was supported by Grants-in-Aid of Scientific Research from the Ministry of Health, Labour, and Welfare of Japan, Grants-in-Aid for Scientific Research from the Ministry of Education, Culture, Sports, Science and Technology of Japan, and Grants-in-Aid of the Japan Science and Technology Agency. The author has no conflict of interest.

ABBREVIATIONS

CAM	=	Cell adhesion molecule
CD	=	Crohn's disease
COX	=	Cyclooxygenase
DAI	=	Disease activity index
DSS	=	Dextran sulfate sodium
GGA	=	Geranylgeranylacetone
HSE	=	Heat shock element
HSP	=	Heat shock protein
IBD	=	Inflammatory bowel disease
ICAM	=	Intercellular adhesion molecule
IL	=	Interleukin
iNOS	=	Inducible NO synthase
LPS	=	Lipopolysaccharide
MPO	=	Myeloperoxidase
NF-kB	=	Nuclear factor kappa B
NO	=	Nitric oxide
NSAID	=	Non-steroidal anti-inflammatory drug
PG	=	Prostaglandin
ROS	=	Reactive oxygen species
S.E.M.	=	Standard error of the mean
TNF	=	Tumor necrosis factor
TUNEL labelling	=	TdT-mediated biotinylated UTP nick end
TNBS	=	Trinitrobenzene sulfonic acid
UC	=	Ulcerative colitis
VCAM	=	Vascular cell adhesion molecule

REFERENCES

[1] Mathew A, Morimoto RI. Role of the heat-shock response in the life and death of proteins. Ann N Y Acad Sci 1998; 851: 99-111.

[2] Morimoto RI. Regulation of the heat shock transcriptional response: cross talk between a family of heat shock factors, molecular chaperones, and negative regulators. Genes Dev 1998; 12: 3788-96.

[3] Hirakawa T, Rokutan K, Nikawa T, Kishi K. Geranylgeranylacetone induces heat shock proteins in cultured guinea pig gastric mucosal cells and rat gastric mucosa. Gastroenterology 1996; 111: 345-57.

[4] Katsuno M, Sang C, Adachi H, Minamiyama M, Waza M, Tanaka F, *et al.* Pharmacological induction of heat-shock proteins alleviates polyglutamine-mediated motor neuron disease. Proc Natl Acad Sci USA 2005; 102: 16801-6.

[5] Tomisato W, Takahashi N, Komoto C, Rokutan K, Tsuchiya T, Mizushima T. Geranylgeranylacetone protects cultured guinea pig gastric mucosal cells from indomethacin.Dig Dis Sci 2000; 45: 1674-9.

[6] Takano T, Tsutsumi S, Tomisato W, Hoshino T, Tsuchiya T, Mizushima T. Geranylgeranylacetone protects guinea pig gastric mucosal cells from gastric stressor-induced apoptosis. Dig Dis Sci 2002; 47: 1546-53.

[7] Tomisato W, Tsutsumi S, Tsuchiya T, Mizushima T. Geranylgeranylacetone protects guinea pig gastric mucosal cells from gastric stressor-induced necrosis by induction of heat-shock proteins. Biol Pharm Bull 2001; 24: 887-91.

[8] Mizushima T, Tsutsumi S, Rokutan K, Tsuchiya T. Suppression of ethanol-induced apoptotic DNA fragmentation by geranylgeranylacetone in cultured guinea pig gastric mucosal cells. Dig Dis Sci 1999; 44: 510-4.

[9] Holzer P. Neural emergency system in the stomach. Gastroenterology 1998; 114: 823-39.

[10] Miller TA. Protective effects of prostaglandins against gastric mucosal damage: current knowledge and proposed mechanisms. Am J Physiol 1983; 245: G601-23.

[11] Terano A, Hiraishi H, Ota S, Sugimoto T. Geranylgeranylacetone, a novel anti-ulcer drug, stimulates mucus synthesis and secretion in rat gastric cultured cells. Digestion 1986; 33: 206-10.

[12] Ushijima H, Tanaka K, Takeda M, Katsu T, Mima S, Mizushima T. Geranylgeranylacetone protects membranes against nonsteroidal anti-inflammatory drugs. Mol Pharmacol 2005; 68: 1156-61.

[13] Tanaka K, Tsutsumi S, Arai Y, Hoshino T, Suzuki K, Takaki E, *et al.* Genetic evidence for a protective role of heat shock factor 1 against irritant-induced gastric lesions. Mol Pharmacol 2007; 71: 985-93.

[14] Suemasu S, Tanaka K, Namba T, Ishihara T, Katsu T, Fujimoto M, *et al.* A role of HSP70 in protecting against indomethacin-induced gastric lesions. J Biol Chem 2009; 284: 19705-15.

[15] Ebert MP, Schafer C, Chen J, Hoffmann J, Gu P, Kubisch C, *et al.* Protective role of heat shock protein 27 in gastric mucosal injury. J Pathol 2005; 207: 177-84.

[16] Cuzzocrea S. Emerging biotherapies for inflammatory bowel disease. Expert Opin Emerg Drugs 2003; 8: 339-47.

[17] Podolsky DK. Inflammatory bowel disease. N Engl J Med 2002; 347: 417-29.

[18] Jurjus AR, Khoury NN, Reimund JM. Animal models of inflammatory bowel disease. J Pharmacol Toxicol Methods 2004; 50: 81-92.

[19] Reinecker HC, Steffen M, Witthoeft T, Pflueger I, Schreiber S, MacDermott RP, *et al.* Enhanced secretion of tumour necrosis factor-alpha, IL-6, and IL-1 beta by isolated lamina propria mononuclear cells from patients with ulcerative colitis and Crohn's disease. Clin Exp Immunol 1993; 94: 174-81.

[20] Danese S, Semeraro S, Marini M, Roberto I, Armuzzi A, Papa A, *et al.* Adhesion molecules in inflammatory bowel disease: therapeutic implications for gut inflammation. Dig Liver Dis 2005; 37: 811-8.

[21] Ludwig D, Stahl M, Ibrahim ET, Wenzel BE, Drabicki D, Wecke A, *et al.* Enhanced intestinal expression of heat shock protein 70 in patients with inflammatory bowel diseases. Dig Dis Sci 1999; 44: 1440-7.

[22] Xie Y, Chen C, Stevenson MA, Auron PE, Calderwood SK. Heat shock factor 1 represses transcription of the IL-1 beta gene through physical interaction with the nuclear factor of interleukin 6. J Biol Chem 2002; 277: 11802-10.

[23] Singh-Jasuja H, Hilf N, Arnold-Schild D, Schild H. The role of heat shock proteins and their receptors in the activation of the immune system. Biol Chem 2001; 382: 629-36.

[24] Tanaka K, Namba T, Arai Y, Fujimoto M, Adachi H, Sobue G, *et al.* Genetic evidence for a protective role for heat shock factor 1 and heat shock protein 70 against colitis. J Biol Chem 2007; 282: 23240-52.

[25] Ohkawara T, Nishihira J, Takeda H, Miyashita K, Kato K, Kato M, *et al.* Geranylgeranylacetone protects mice from dextran sulfate sodium-induced colitis. Scand J Gastroenterol 2005; 40: 1049-57.

[26] Ohkawara T, Nishihira J, Takeda H, Katsurada T, Kato K, Yoshiki T, *et al.* Protective effect of geranylgeranylacetone on trinitrobenzene sulfonic acid-induced colitis in mice. Int J Mol Med 2006; 17: 229-34.

[27] Sun D, Chen D, Du B, Pan J. Heat shock response inhibits NF-kappaB activation and cytokine production in murine Kupffer cells. J Surg Res 2005; 129: 114-21.

[28] Guzhova IV, Darieva ZA, Melo AR, Margulis BA. Major stress protein Hsp70 interacts with NF-kB regulatory complex in human T-lymphoma cells. Cell Stress Chaperones 1997; 2: 132-9.

[29] Chan JY, Ou CC, Wang LL, Chan SH. Heat shock protein 70 confers cardiovascular protection during endotoxemia via inhibition of nuclear factor-kappaB activation and inducible nitric oxide synthase expression in the rostral ventrolateral medulla. Circulation 2004; 110: 3560-6.

[30] Pahl HL. Activators and target genes of Rel/NF-kappaB transcription factors. Oncogene 1999; 18: 6853-66.

[31] Chen H, Wu Y, Zhang Y, Jin L, Luo L, Xue B, *et al.* Hsp70 inhibits lipopolysaccharide-induced NF-kappaB activation by interacting with TRAF6 and inhibiting its ubiquitination. FEBS Lett 2006; 580: 3145-52.

[32] Collins T. Endothelial nuclear factor-kappa B and the initiation of the atherosclerotic lesion. Lab Invest 1993; 68: 499-508.

[33] Nakabe N, Kokura S, Shimozawa M, Katada K, Sakamoto N, Ishikawa T, *et al.* Hyperthermia attenuates TNF-alpha-induced up regulation of endothelial cell adhesion molecules in human arterial endothelial cells. Int J Hyperthermia 2007; 23: 217-24.

[34] Maiden L, Thjodleifsson B, Seigal A, Bjarnason II, Scott D, Birgisson S, *et al.* Long-term effects of nonsteroidal anti-inflammatory drugs and cyclooxygenase-2 selective agents on the small bowel: a cross-sectional capsule enteroscopy study. Clin Gastroenterol Hepatol 2007; 5: 1040-5.

[35] Lanas A, Ferrandez A. NSAID-induced gastrointestinal damage: current clinical management and recommendations for prevention. Chin J Dig Dis 2006; 7: 127-33.

[36] Graham DY, Opekun AR, Willingham FF, Qureshi WA. Visible small-intestinal mucosal injury in chronic NSAID users. Clin Gastroenterol Hepatol 2005; 3: 55-9.

[37] Morris AJ, Madhok R, Sturrock RD, Capell HA, MacKenzie JF. Enteroscopic diagnosis of small bowel ulceration in patients receiving non-steroidal anti-inflammatory drugs. Lancet 1991; 337: 520.

[38] Sigthorsson G, Simpson RJ, Walley M, Anthony A, Foster R, Hotz-Behoftsitz C, *et al.* COX-1 and 2, intestinal integrity, and pathogenesis of nonsteroidal anti-inflammatory drug enteropathy in mice. Gastroenterology 2002; 122: 1913-23.

[39] Somasundaram S, Sigthorsson G, Simpson RJ, Watts J, Jacob M, Tavares IA, *et al.* Uncoupling of intestinal mitochondrial oxidative phosphorylation and inhibition of cyclooxygenase are required for the development of NSAID-enteropathy in the rat. Aliment Pharmacol Ther 2000; 14: 639-50.

[40] Basivireddy J, Vasudevan A, Jacob M, Balasubramanian KA. Indomethacin-induced mitochondrial dysfunction and oxidative stress in villus enterocytes. Biochem Pharmacol 2002; 64: 339-49.

[41] Wallace JL. The 1994 Merck Frosst Award. Mechanisms of nonsteroidal anti-inflammatory drug (NSAID) induced gastrointestinal damage--potential for development of gastrointestinal tract safe NSAIDs. Can J Physiol Pharmacol 1994; 72: 1493-8.

[42] Konaka A, Kato S, Tanaka A, Kunikata T, Korolkiewicz R, Takeuchi, K. Roles of enterobacteria, nitric oxide and neutrophil in pathogenesis of indomethacin-induced small intestinal lesions in rats. Pharmacol Res 1999; 40: 517-24.

[43] Whittle BJ, Laszlo F, Evans SM, Moncada S. Induction of nitric oxide synthase and microvascular injury in the rat jejunum provoked by indomethacin. Br J Pharmacol 1995; 116: 2286-90.

[44] Jacob M, Foster R, Sigthorsson G, Simpson R, Bjarnason I. Role of bile in pathogenesis of indomethacin-induced enteropathy. Arch Toxicol 2007; 81: 291-8.

[45] Goldstein JL, Eisen GM, Lewis B, Gralnek IM, Aisenberg J, Bhadra P, *et al.* Small bowel mucosal injury is reduced in healthy subjects treated with celecoxib compared with ibuprofen plus omeprazole, as assessed by video capsule endoscopy. Aliment Pharmacol Ther 2007; 25: 1211-22.

[46] Aabakken L, Bjornbeth BA, Weberg R, Viksmoen L, Larsen S, Osnes M. NSAID-associated gastroduodenal damage: does famotidine protection extend into the mid- and distal duodenum? Aliment Pharmacol Ther 1990; 4: 295-303.

[47] Urayama S, Musch MW, Retsky J, Madonna MB, Straus D, Chang EB. Dexamethasone protection of rat intestinal epithelial cells against oxidant injury is mediated by induction of heat shock protein 72. J Clin Invest 1998; 102: 1860-5.

[48] Asano T, Tanaka K, Yamakawa N, Adachi H, Sobue G, Goto H, *et al.* Hsp 70 confers protection against indomethacin-induced lesions of the small intestine. J Pharmacol Exp Ther 2009; 330: 458-67.

Received: December 9, 2009 **Accepted: January 10, 2010**

Biol. Pharm. Bull.

Regular Article

Molecular and Cell Biology

Low Direct Cytotoxicity of Loxoprofen on Gastric Mucosal Cells

Naoki YAMAKAWA, Shintaro SUEMASU, Ayumi KIMOTO, Yasuhiro ARAI, Tomoaki ISHIHARA, Kazumi YOKOMIZO, Yoshinari OKAMOTO, Masami OTSUKA, Ken-ichiro TANAKA and Tohru MIZUSHIMA*

Graduate School of Medical and Pharmaceutical Sciences, Kumamoto University, Kumamoto 862-0973, Japan

*To whom correspondence should be addressed. e-mail: mizu@gpo.kumamoto-u.ac.jp

Abstract

Pro-drugs of non-steroidal anti-inflammatory drugs (NSAIDs), such as loxoprofen are widely used for clinical purposes because they are not so harmful to the gastrointestinal mucosa. We recently showed that NSAIDs such as indomethacin and celecoxib have direct cytotoxicity (ability to induce necrosis and apoptosis in gastric mucosal cells) due to their membrane permeabilizing activities, which is involved in NSAID-induced gastric lesions. We show here that under conditions where indomethacin and celecoxib clearly induce necrosis and apoptosis, loxoprofen and its active metabolite loxoprofen-OH, do not have such effects in primary culture of guinea pig gastric mucosal cells. Loxoprofen and loxoprofen-OH induced apoptosis more effectively in cultured human gastric cancer cells than in the primary culture. Loxoprofen and loxoprofen-OH exhibited much lower membrane permeabilizing activities than did indomethacin and celecoxib. We thus consider that the low direct cytotoxicity of loxoprofen observed *in vitro* is involved in its relative safety on production of gastric lesions in clinical situation.

Key Words: loxoprofen; gastric mucosal cells; membrane permeabilization; gastric lesions

INTRODUCTION

Non-steroidal anti-inflammatory drugs (NSAIDs), such as indomethacin, are a useful family of therapeutics.[1)] An inhibitory effect of NSAIDs on cyclooxygenase (COX) activity is responsible for their anti-inflammatory actions because COX is an enzyme essential for the synthesis of prostaglandins (PGs), such as PGE_2, which have a strong capacity to induce inflammation. On the other hand, NSAID use is associated with gastrointestinal complications.[2-4)]

In 1991, two subtypes of COX, COX-1 and COX-2, which are responsible for the majority of COX activity at the gastrointestinal mucosa and in tissues with inflammation, respectively, were identified.[5,6)] Since PGE_2 has a strong protective effect on the gastrointestinal mucosa, it is reasonable to speculate that selective COX-2 inhibitors maintain anti-inflammatory activity without gastrointestinal side-effects. In fact, a greatly reduced incidence of gastroduodenal lesions has been reported for selective COX-2 inhibitors (such as celecoxib and rofecoxib).[7-9)] However, a recently raised issue concerning the use of selective COX-2 inhibitors is their potential risk for cardiovascular thrombotic events.[10,11)] This may be due to the fact that prostacyclin, a potent anti-aggregator of platelets and a vasodilator, is mainly produced by COX-2 in vascular endothelial cells, while thromboxane A_2, a potent aggregator of platelets and a vasoconstrictor, is mainly produced by COX-1 in platelets.[12-14)] Because of this concern, rofecoxib was withdrawn from the worldwide market. Therefore, NSAIDs exhibiting gastrointestinal safety, other than selective COX-2 inhibitors, are clinically important.

The inhibition of COX by NSAIDs is not the sole explanation for the gastrointestinal side-effects of NSAIDs.[15] We have recently demonstrated that NSAIDs induce necrosis and apoptosis in cultured gastric mucosal cells and at gastric mucosa in a manner independent of COX inhibition.[16-20] We clearly showed that the primary target of NSAIDs for induction of necrosis and apoptosis is cytoplasmic membranes.[16,18] As for the molecular mechanism governing this apoptosis, we have proposed the following pathway. Permeabilization of cytoplasmic membranes by NSAIDs stimulates Ca^{2+} influx and increases intracellular Ca^{2+} levels, which in turn induces the endoplasmic reticulum (ER) stress response.[16,21,22] In this response, an apoptosis-inducing transcription factor, C/EBP homologous transcription factor (CHOP), is induced and CHOP induces expression of p53 up-regulated modulator of apoptosis (PUMA) and resulting translocation and activation of Bax, mitochondrial dysfunction, activation of caspases and apoptosis.[17,23] Furthermore, we have suggested that both COX inhibition and gastric mucosal cell death are required for the formation of NSAID-induced gastric lesions *in vivo*.[20,24]

Loxoprofen has been used clinically for a long time as a standard NSAID in Japan, and clinical studies have suggested that it is safer than other NSAIDs, such as indomethacin.[25,26] Loxoprofen is a pro-drug, which is converted (by reduction of the cyclopentanone moiety) to its active metabolite (the *trans*-alcohol metabolite of loxoprofen, loxoprofen-OH) by aromatic aldehyde-ketone reductase only after absorption by the gastrointestinal tract.[27] However, the direct cytotoxicity and membrane permeabilization activity of loxoprofen has not been tested. In this study, we found that loxoprofen and loxoprofen-OH have relatively lower membrane permeabilization activities and cytotoxic

effects on gastric mucosal cells than other NSAIDs. Based on these observations, we consider that the low direct cytotoxicity of loxoprofen will render its use clinical safe on the gastrointestinal mucosa.

MATERIALS AND METHODS

Chemicals and media

RPMI 1640 was obtained from Nissui Pharmaceutical Co. Fetal bovine serum (FBS) and 3-(4, 5-dimethyl-thiazol-2-yl)-2, 5-diphenyl tetrazolium bromide (MTT) were from Sigma Co. Loxoprofen and loxoprofen-OH were kindly gifted from Daiichi-Sankyo Co. Indomethacin was from Wako Co. Celecoxib was from LKT Laboratories Inc. Egg phosphatidylcholine (PC) was from Kanto Chemicals Co. Male guinea pigs weighing 200-300 g were purchased from Kyudo Co. The experiments and procedures described here were carried out in accordance with the Guide for the Care and Use of Laboratory Animals as adopted and promulgated by the National Institute of Health and were approved by the Animal Care Committee of Kumamoto University.

In vitro assay of cytotoxicity of NSAIDs and COX-inhibition

Gastric mucosal cells were isolated from guinea pig fundic glands as described previously.[28,29] Isolated gastric mucosal cells were cultured for 12 h in RPMI 1640 containing 0.3% v/v FBS, 100 U/ml ampicillin and 100 μg/ml streptomycin in type-I collagen-coated plastic culture plates under the conditions of 5% CO_2/95% air and 37°C. After removing non-adherent cells, cells attached to the plate were used. Guinea pig gastric mucosal cells prepared under these conditions were previously characterized, with the

majority (about 90%) of cells being identified as pit cells.[28,30] Human gastric adenocarcinoma (AGS) cells were cultured on plastic culture plates without collagen-coating under the same conditions.

NSAIDs were dissolved in DMSO. Cells were exposed to NSAIDs by changing the entire bathing medium.

We used MTT assay for monitoring cell viability. Cells were incubated for 2 h with MTT solution at a final concentration of 0.5 mg/ml. Isopropanol and hydrochloric acid were added to the culture medium at final concentrations of 50% and 20 mM, respectively. The optical density of each sample at 570 nm was determined spectrophotometrically using a reference wavelength of 630 nm.[31]

The amount of PGE_2 in the medium was determined using an EIA kit (Cayman, Ann Arbor, MI) according to the manufacturer's protocol.

Apoptotic DNA fragmentation was monitored as previously described [31]. Cells were collected using a rubber policeman and suspended in 20 μl of lysis buffer, consisting of 50 mM Tris-HCl (pH7.8), 10 mM EDTA, and 0.5% sodium-N-lauroylsarcosinate. Proteinase K was added to a final concentration of 1 mg/ml, and the lysate was incubated at 50°C for 2 hours. RNaseA was then added to a final concentration of 0.5 mg/ml and incubated at 50°C for 30 min. These samples were analyzed by 2% agarose gel electrophoresis in the presence of 0.5 μg/ml ethidium bromide.

Apoptotic chromatin condensation was monitored as described previously [31]. Cells were washed with PBS, stained with 10 μg/ml Ho 342 and observed under a fluorescence microscope.

Membrane permeability assay

Membrane permeability assays were performed as described previously.[16,18,32] Liposomes were prepared using the reversed-phase evaporation method. Egg PC (10 μmol, 7.7 mg) was dissolved in chloroform/methanol (1:2, v/v), dried, and dissolved in 1.5 ml of diethyl ether. This was followed by the addition of 1 ml of 100 mM calcein-NaOH (pH 7.4). The mixture was sonicated to obtain a homogenous emulsion. The diethyl ether solvent was removed using a conventional rotary evaporator under reduced pressure at 25°C. The resulting suspension of liposome was centrifuged and washed twice with fresh buffer A (10 mM phosphate buffer, containing 150 mM NaCl) to remove untrapped calcein. The final liposome precipitate was re-suspended in 5 ml buffer A. A 0.3 ml aliquot of this suspension was diluted with 19.7 ml of buffer A, following which 400 μl of this suspension was incubated at 30°C for 10 min in the presence of the NSAID under investigation. The release of calcein from liposomes (the amount of calcein outside the liposomes) was determined by measuring fluorescence intensity at 520 nm (excitation at 490 nm), because the calcein fluoresces very weakly when at high concentrations (when calcein is trapped in liposomes) due to self-quenching.

Hemolysis in erythrocytes were monitored as described [33,34] with some modifications. Rat erythrocytes were washed twice with buffer A (5 mM HEPES/NaOH (pH 7.4) and 150 mM NaCl) and then suspended in fresh buffer A at a final concentration of 0.5% hematocrit (5 x 10^7 cells/ml). After incubation with NSAIDs for 10 min at 30°C,